AVALANCHE PHOTODIODES FOR THE CMS ELECTROMAGNETIC CALORIMETER

B. Patel, R. Rusack, P. Vikas(email:Pratibha.Vikas@cern.ch)
University of Minnesota, Minneapolis, U.S.A.
Y. Musienko*, S. Nicol, S.Reucroft, J. D. Swain
Northeastern Univeristy, Boston, U.S.A.
K. Deiters, D. Renker, T. Sakhelashvili
PSI, Villigen, Switzerland

Abstract

Avalanche photodiodes(APD's) will be used as photodetectors in the CMS barrel electromagnetic crystal calorimeter for high precision energy measurements in a hostile radiation environment. Significant progress has been made in the characteristics of these devices being expressly developed for CMS. Parameters of the final structure APD's together with demonstrations of radiation hardness and plans for quality assurance/control during the production phase are presented.

1. INTRODUCTION

In order to optimise the potential for discovering the Higgs, supersymmetry and other possible new physics and study a large variety of standard model processes, CMS requires a high performance electromagnetic calorimeter (ECAL)[1]. The CMS ECAL barrel will be made of 61200 lead tungstate ($PbWO_4$) crystals. $PbWO_4$ is a fast and compact scintillating crystal with peak scintillation emisssion around 420-450 nm. However, lead tungstate has a relatively low light yield which necessitated the use of a photodetector with a small nuclear counter effect, i.e., a small fake signal from ionising particles. It has to operate with a high quantum efficiency for the peak scintillation of $PbWO_4$ in a rather hostile environment with a strong 4T magnetic field and unprecedented radiation levels. Avalanche photodiodes (APD's) satisfy all these criteria and they will be used as photodetectors in a large scale HEP experiment for the first time in the CMS ECAL barrel. Each crystal will be equipped with two large surface (5x5 mm^2 area) APD's operated at a gain of 50.

The resolution of an electromagnetic calorimeter can be expressed as:

$$\frac{\sigma_E}{E} = \frac{a}{\sqrt{E(GeV)}} + b + \frac{c}{E},$$

where the stochastic term a is due to the intrinsic shower fluctuations combined with the photostatistics contribution, the constant term b is related to the stability and reproducibility of the detector and c is the noise contribution due to electronics, pile-up etc. The APD's contribute to all three terms. Since, avalanche photomultiplication is a stochastic process, the so called excess noise factor, F, contributes to a. Gain variations with bias voltage and temperature contribute to the constant term b. The APD capacitance and dark current contribute to c. Therefore, aside from matching the properties of $PbWO_4$, it is also imperative to optimise all these parameters for the APD's destined for use in the CMS ECAL .

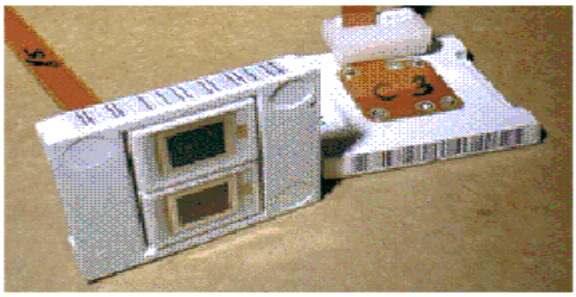

Figure 1: Two APD's mounted in a supporting structure, which is glued onto the crystal rear end.

Two companies EG&G in Canada and Hamamatsu Photonics in Japan started the development work on APD's suitable for use in the CMS ECAL in 1995 and some thirty prototypes were tested. The choice between the two vendors was made in favour of Hamamatsu in July 1998. Subsequently, an R&D contract was signed with Hamamatsu for further development. Currently, we are in the final stages of the development phase and a decision on the final APD structure was made in July 1999. Hamamatsu Photonics has developed an APD, which is well suited for this demanding application. Results from the measurements of 180 devices of this

* On leave from INR (Moscow).

type performed at a quality assurance/quality control facility at CERN and irradiations at PSI are presented. The plans for quality assurance/quality control during the production phase are also discussed.

2. PROPERTIES OF THE SELECTED APD

Figure 1 is a picture of two APD's mounted in a supporting structure which is glued onto the crystal rear end. Hamamatsu APD's are made by epitaxial growth on low resistivity N+ silicon followed by ion implantation and diffusion. A schematic diagram of the chosen structure is shown in Figure 2. The P material in front of the amplification region, the P-N junction, is made less than 10 μm thick to reduce the sensitivity to ionising radiation. The N^- layer is introduced to reduce the capacitance and the dependence of the gain on the bias voltage. The V-shaped grooves, which are some 50 μm deep and wide, help to suppress the surface currents.

2.1 Stability of the Gain with bias voltage and temperature

Gain is determined in DC mode by measurements of the differences in current when the APD is illuminated by a blue LED(420 nm) and the dark currents[1]. Figure 3 is a representative distribution of gain versus bias voltage for these APD's. The dependence of the gain, M, on the bias voltage is rather steep in the region of interest, i.e., M=50. The average operating voltage for a gain of 50 for these APD's is ~330V with a 20V spread. Since, a group of APD's will be biased by the same power supply,

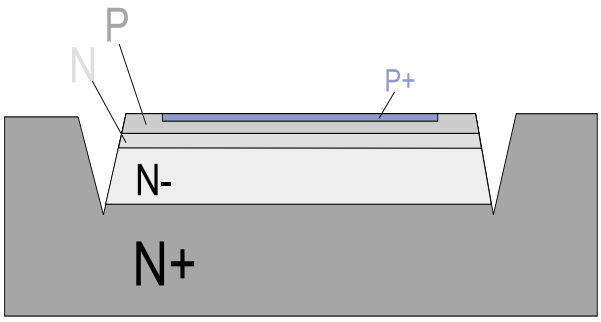

Figure 2: Structure of the selected APD.

Hamamatsu is trying to reduce this spread in the ongoing, fine-tuning phase.

The average variation of gain with the bias voltage,1/M* dM/dV, has been found to be 3.3% for these devices. This is a great improvement compared to the earlier prototypes[2].

The gain depends on the temperature. This dependence, 1/M*dM/dT, has been measured to be –2.2%/°C at a gain of 50, as shown in Figure 4. Lead tungstate crystals have the same temperature coefficient and hence, the detector temperature has to be stabilised to a tenth of a degree in any case.

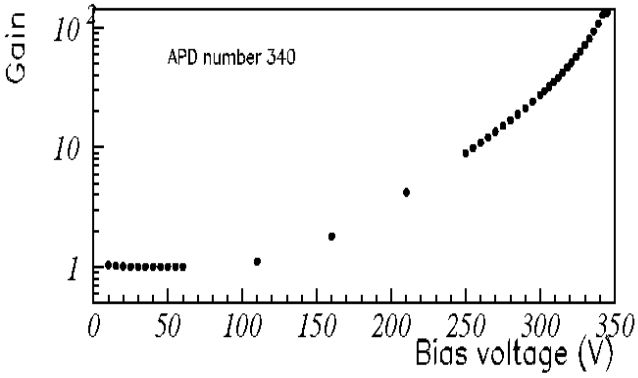

Figure 3: APD gain versus bias voltage for an APD.

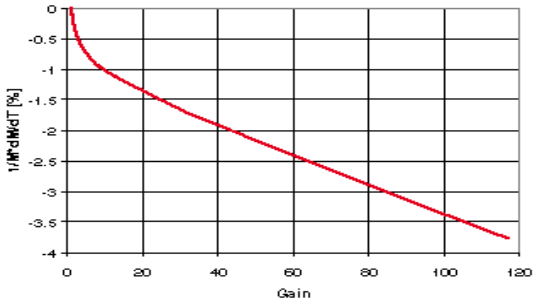

Figure 4: The temperature coefficient of the gain versus the gain for an APD.

2.2 Dark Current

These APD's have very low dark current and the dark current for gain 50 is less than 10 nA for most of them. Figure 5 shows the dark current for all the 180 devices.

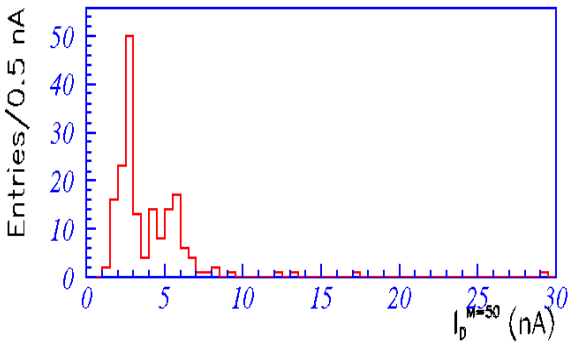

Figure 5: Dark current for gain 50 for all the APD's.

2.3 Nuclear Counter Effect

Minimum ionising particles from the rare leakage of an electromagnetic shower create some 100 electron-hole pairs/μm in Si but only those electrons that are created in front of the P-N junction can start an avalanche. Since, light produces electrons close to the surface, all will be amplified in an avalanche. The nuclear counter effect , the electrical signal generated by the passage of ionising radiation through the APD, can be quantified in terms of the effective thickness of a silicon PIN diode with the same response to electrons from a source and can be defined as:

$$l_{eff} = \frac{(\text{peak position})_{APD}}{(\text{peak position})_{PIN}} \times \frac{200\mu m}{M}$$

where M is the gain of the APD and the PIN diode used in this case is 200 μm thick. Figure 6 shows the resulting pulse height spectra for an APD and a PIN diode which gives I_{eff}=5.6 μm.

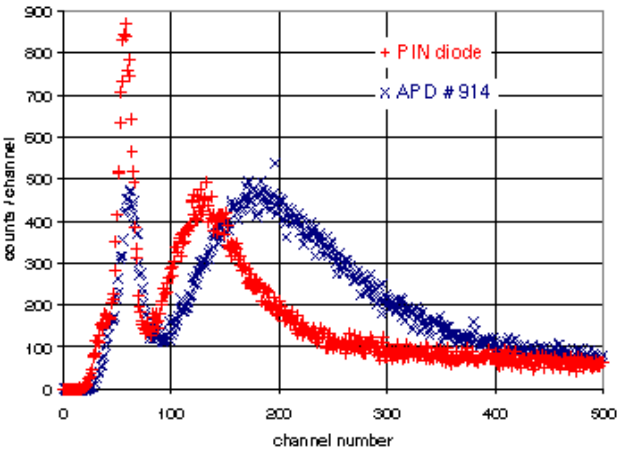

Figure 6: APD and PIN diode response to electrons from a ^{90}Sr source.

2.4 Excess Noise Factor

The fluctuations in avalanche multiplication are characterised by the excess noise factor, *F* which can be approximated by the following expression[3] at high gain:

$$F = k \times M + \left(2 - \frac{1}{M}\right) \times (1 - k)$$

where, k is the ratio of the ionisation coefficients for holes and electrons. The excess noise factor for these APD's has been measured to be ~2 for a gain of 50, as shown in Figure 7.

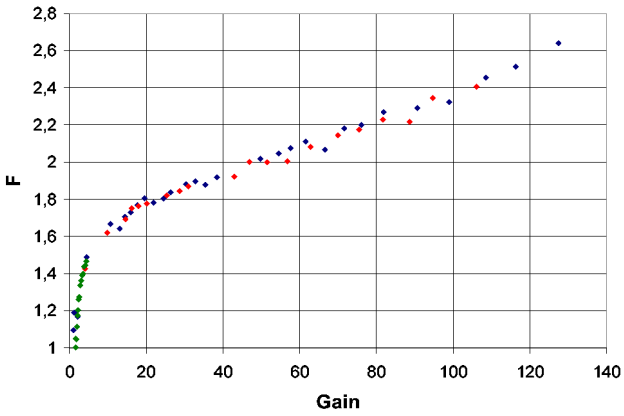

Figure 7: The excess noise factor as a function of APD gain

3. EFFECT OF IRRADIATION

Radiation damage on APD's occurs via two mechanisms:

1) surface damage which causes defects in the front layer, increasing the surface dark current and reducing the quantum efficiency.

2) bulk damage due to the displacement of atoms from their lattice sites increasing the bulk dark current and potentially changing the gain for a given bias.

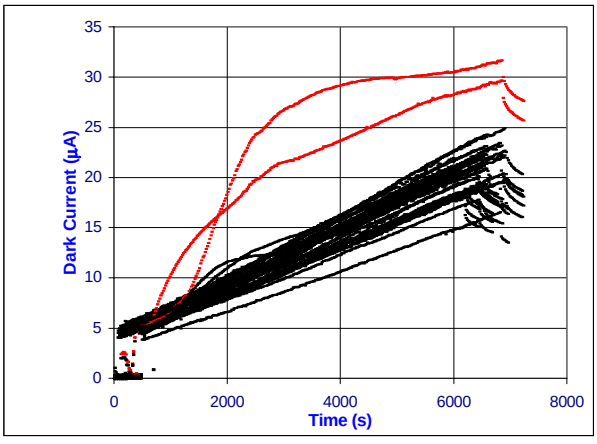

Figure 8: Dark current versus irradiation time.

Forty APD's were irradiated at PSI in a 72 MeV proton beam. They were exposed to the beam for approximately 105 minutes which corresponds to a total 1 MeV neutron flux of $2*10^{13}$ neutrons/cm^2[4]. This is equivalent to the fluence expected in the CMS barrel for 10 years of operation. Figure 8 shows the currents (dark and

ionisation) for the forty APD's during irradiation as a function of time in the beam in seconds. All except two APD's showed no anomaly during the irradiation. There was a steep rise of the currents for these two. The position on the wafer for this batch of APD's is known and these two APD's came from the edge of the wafer. Clearly, the APD's from the edges of wafers will have to be discarded during production.

The irradiated APD's were then annealed for one week at 90°C and all their parameters remeasured to ascertain the damage due to irradiation.

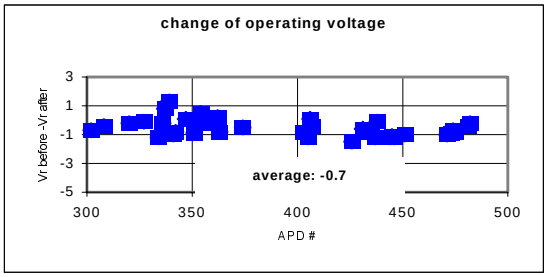

Figure 9: Change in bias voltage for a gain of 50 with irradiation versus the APD number.

Figure 9 shows the change in the bias voltage with irradiation for a gain of 50 versus the APD number. The average change was -0.7 V which corresponds to ~2% reduction in the gain for a given bias.

Figure 10 shows the change in the distance to the breakdown voltage from the bias voltage for a gain of 50 (breakdown is defined as the voltage when the dark current is 100 µA) for the irradiated APD's versus the APD number. The change in the breakdown voltage is large for these APD's. This is one of the APD properties being improved during the ongoing fine tuning phase. The two APD's which have 0 and 5 V distance to breakdown are the same as the ones with high currents during irradiation.

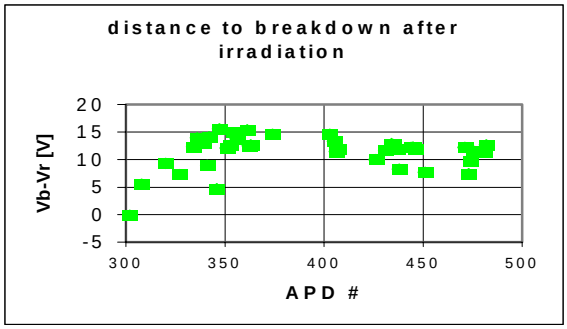

Figure 10: The distance to breakdown voltage from the operating voltage versus the APD number for irradiated APD's.

Figure 11 shows the dark current versus the APD number for the irradiated APD's measured at 25°C. The average

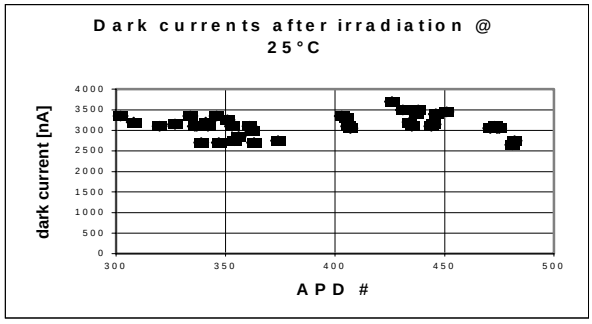

Figure 11: Dark current post-irradiation versus the APD number

dark current is ~3µA. It should be noted that at 18°C, the nominal temperature CMS will operate in, the dark current will be half of this. This translates to a noise contribution of 170 MeV due to the APD leakage current after 10 years of LHC operation.

Figure 12 shows the change in quantum efficiency post-irradiation versus wavelength for four of these APD's. The quantum efficiency remains the same for the wavelengths of interest, i.e., 400-500 nm and a reduction is only seen for wavelengths larger than 600 nm. These measurements were performed with the APD at gain 1.

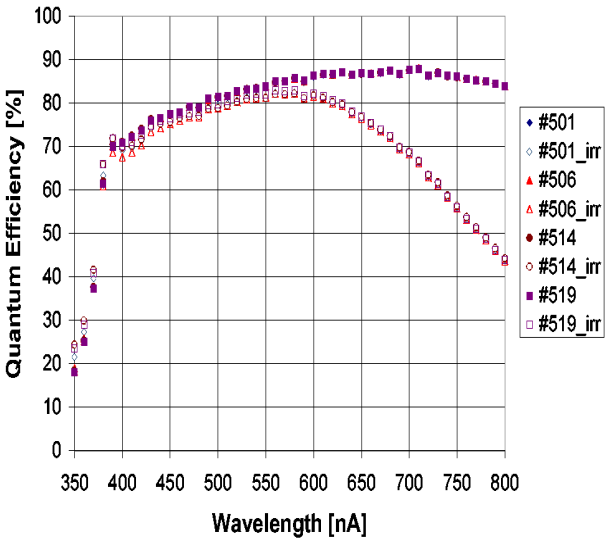

Figure 12: Quantum efficiency before and after irradiation versus the wavelength.

It was confirmed that all the other parameters for these irradiated APD's remained the same within measurement errors.

4. APD QUALITY ASSURANCE AND QUALITY CONTROL

In order to ensure and control the quality of APD's delivered during the production phase, a facility capable of fully characterising these devices has been set up at CERN. Radiation hardness tests will continue to be performed at PSI and a new facility with a ^{252}Cf source, currently being set up at the University of Minnesota. On receiving a new wafer, the vendor will initially only package 2% of the devices from it and send them to PSI or Minnesota where they will be irradiated. The packaging of the rest of the APD's derived from a given wafer will proceed if and only if all of the 2% successfully meet our radiation hardness criteria. In addition, another 2% of the devices will be subject to other destructive tests like long term aging at CERN.

Hamamatsu will provide measurements of the gain curves, dark currents and the quantum efficiency at a given wavelength for all the devices using a set up designed by us. These measurements will be done at 25°C. The quality assurance/control facility at CERN will measure these devices on a sampling basis to track the Hamamatsu measurements. In addition, more detailed tests of production APD's will also be performed on a sampling basis to track the production process as a whole.

The quality assurance/control facility at CERN became functional in April 1999 and will continue to do so till the end of production. In addition, the APD's will also be fully characterised after mounting in the supporting structure which will be glued on the crystals, initially in Lyon and then at CERN.

5. CONCLUSIONS

Intensive R&D has led to the development of APD's by Hamamatsu Photonics which are suitable for use in the CMS ECAL. The important parameters of these APD's are summarised in Table 1. These APD's have a small nuclear counter effect, low excess noise factor, low capacitance and they can withstand the radiation levels expected in the CMS barrel while maintaining the performance CMS is aiming for. The remaining concerns with these devices are the spread in the bias voltage for the operating gain of 50 and the change in the breakdown voltage with irradiation. The structure and manufacturing technology for these devices is being ``fine tuned'' by the vendor at the moment and these problems are being addressed. The final decision on the structure and manufacturing technology will be made in Oct 1999 and production will commence in Dec 1999. We expect to receive the first production devices in Jan 2000.

A facility capable of fully characterising APD's for quality assurance/control is in place at CERN and fully functional. The testing for radiation hardness of these devices will continue at PSI and Minnesota.

Active Area	5x5 mm^2
Operating voltage	~330 V
Capacitance	70 pF
Serial resistance	3 Ω
Dark current	< 10 nA
Quantum efficiency	72% @ 420 nm
1/M*dM/dV (M=50)	3.3%
1/M*dM/dT (M=50)	-2.2%

Table 1: Summary of APD parameters.

6. REFERENCES

[1] The Electromagnetic Calorimeter Project, Technical Design Report, CERN/LHCC97-31(1997).

[2] A. Karar et al, NIM A428 (1999) 413.

[3] T. Kirn et al, NIM A387 (1997) 199.
F. Cavallari, NIM A409(1998) 564.

[4] R. McIntyre, IEEE Trans. Electron Dev. ED-19 (1972) 703.

[5] M. Huhtinen and P. Aarnio, NIM A 335 (1993) 580.